Integral equations for simple fluids in a general reference functional approach

2005 J. Phys.: Condens. Matter 17 429

(http://iopscience.iop.org/0953-8984/17/3/003)

INSTITUTE OF PHYSICS PUBLISHING JOURNAL OF PHYSICS: CONDENSED MATTER

J. Phys.: Condens. Matter **17** (2005) 429–452 doi:10.1088/0953-8984/17/3/003

Integral equations for simple fluids in a general reference functional approach

M Oettel

Max-Planck-Institut für Metallforschung, Heisenbergstrasse 3, 70569 Stuttgart, Germany
and
Institut für Theoretische und Angewandte Physik, Universität Stuttgart, Pfaffenwaldring 57, 70569 Stuttgart, Germany

E-mail: oettel@mf.mpg.de

Received 14 October 2004, in final form 12 November 2004
Published 7 January 2005
Online at stacks.iop.org/JPhysCM/17/429

Abstract

The integral equations for the correlation functions of an inhomogeneous fluid mixture are derived using a functional Taylor expansion of the free energy around an inhomogeneous equilibrium distribution. The system of equations is closed by the introduction of a reference functional for the correlations beyond second order in the density difference from the equilibrium distribution. Explicit expressions are obtained for energies required to insert particles of the fluid mixture into the inhomogeneous system. The approach is illustrated by the determination of the equation of state of a simple, truncated Lennard-Jones fluid and the analysis of the behaviour of this fluid near a hard wall. The wall–fluid integral equation exhibits complete drying and the corresponding coexisting densities are in good agreement with those obtained from the standard (Maxwell) construction applied to the bulk fluid. The self-consistency of the approach is examined by analysing the virial/compressibility routes to the equation of state and the Gibbs–Duhem relation for the bulk fluid, and the contact density sum rule and the Gibbs adsorption equation for the hard-wall problem. For the bulk fluid, we find good self-consistency for stable states outside the critical region. For the hard-wall problem, the Gibbs adsorption equation is fulfilled very well near phase coexistence where the adsorption is large. For the contact density sum rule, we find deviations of up to 20% in the ratio of the contact densities predicted by the present method and predicted by the sum rule. These deviations are largely due to a slight disagreement between the coexisting density for the gas phase obtained from the Maxwell construction and from complete drying at the hard wall.

(Some figures in this article are in colour only in the electronic version)

1. Introduction

Integral equations have become a popular and increasingly accurate tool in describing the thermodynamics and the bulk structure of one-component simple liquids and, to a smaller degree of accuracy, of fluid mixtures. In the early, formal work (see [1–3] and references therein) the structural ingredients (pair correlation function, direct correlation function and bridge function) were defined in terms of graphical expansions and two exact equations relating these three functions have been established. The unknown third equation which is necessary for a closed system of equations is usually referred to as the closure relation. A number of approximations have been developed in the past for the closure relation. Some of the more successful ones for the structure and thermodynamics of a one-component liquid are the optimized random phase approximation (ORPA) [4], the hierarchical reference theory (HRT) [5], the self-consistent Ornstein–Zernike approximation (SCOZA) [6], the Martynov–Sarkisov closure [7] and the reference hypernetted chain equations (RHNC) [8]. For a general introduction to the subject treating some of these and other common closures, see [9]. The extension of integral equation theories to a general inhomogeneous system defined by an external potential (a wall, say) is possible by incorporating the source of inhomogeneity as a second component in the dilute limit (the wall particle) and treating the originally inhomogeneous problem as a bulk (homogeneous) problem in the two-component mixture. This generalization fails for all of the above closures whenever the phenomenon of wetting in the presence of the external (wall) potential is involved.

On the one hand this failure is linked to the difficulties of defining the free energy and chemical potential accurately and consistently in the two-component (wall–fluid) mixture. Or, whenever a free energy approximation underlying a certain closure relation can be formulated, its form does not allow for wetting. For example, it can be proved that in the hard-wall case the HNC and RHNC closures miss the phenomenon of complete drying for the above reason (for HNC, the proof is given in [10] and it can be easily extended to RHNC). This problem was tackled tentatively in [11, 12] in what is termed the hydrostatic HNC approach and this will be commented on in section 3.3.

On the other hand, one is inclined to link this failure to the difficulty of incorporating the wall as a second component. As the formal framework embodied in the graphical expansions holds equally well for a general inhomogeneous situation, one may abandon the mixture idea and study the one-component fluid using the common closure relations but now for the inhomogeneous correlation functions. These are defined in the presence of an external potential which necessarily entails a loss of symmetry for the correlation functions and thus results in a noticeable increase in computational power required for a numerical solution. Nevertheless, the problem of defining the chemical potential in the inhomogeneous situation still persists; for a review of possible solutions for a range of commonly used closures see [13]. Away from phase transitions, inhomogeneous integral equation closures may give very accurate density profiles; for the example of a fluid confined in a slit see [14]. However, systematic studies of wetting and drying phenomena within this approach have remained fragmentary; see [15–18]. Very recently and quite distinct from the usual closures, an implementation of HRT for the inhomogeneous problem has been presented in [19].

Parallel to the development of integral equation approaches, density functional models have become established as a widespread tool for the investigation of inhomogeneous fluids and for the study of wetting phenomena, in particular. The first study of the latter using a ‘modern’ density functional theory has been reported in [20]; for a summary of the initial development of the field see [21]. In contrast to integral equations, a very simple mean-field type of functional (with a local and therefore actually quite inadequate treatment of

the sharply repulsive interatomic potentials) predicts rich wetting phenomena at walls; see e.g. [22, 23]. This is related to the underlying bulk equation of state which can be derived from the mean-field functional: it is a reasonable zeroth-order approximation to the true equation of state. The drawback of the simplest models of the type discussed in [22, 23] consists in their complete failure to describe realistically fluid correlation functions. This is due to the inadequate treatment of the short-range repulsive forces. By now the treatment of short-ranged correlations within hard-sphere density functionals has reached a very satisfactory level of precision and internal consistency; for landmark developments see [24–26]. By contrast, the treatment of the attractive tails in the interatomic potentials has remained on the mean-field level which leaves the equation of state treated in zeroth-order approximation.

In order to relate density functional results in the presence of a wall, say, to quasi-exact results as obtained from simulations, a number of methods have been proposed. First, one can observe that away from the critical region, density functional results accurately reproduce simulation results if the mean-field coexistence curve is appropriately scaled [27]. Second, close to exact correlation functions obtained from integral equation methods may be used as input in density functionals; see [28–30]. These amendments generally improve the agreement between density profiles obtained from theory and simulation. However, by introducing these *ad hoc* modifications some key properties of the basic functionals (hard-sphere functional plus mean-field treatment of attractions) are destroyed such as the compliance with the results of exact sum rules. Additionally, if this modified class of density functionals is applied to reproduce the bulk fluid correlation functions (this so-called test particle limit is obtained by choosing the fluid interatomic potential as the external potential) there is, in general, no agreement between the integral equation input and the density functional output.

This requirement of test particle consistency was the starting point for the density functional theory developed in [31] which tries to combine standard density functional and integral equation approaches more consistently. By making a Taylor expansion of the free energy functional around bulk densities the standard bulk integral equations are derived and the bridge function in the bulk is determined via a density functional for a suitably chosen reference system of hard spheres, thereby providing the necessary closure relation. The latter resembles the RHNC closure. Results for the bulk structure of the one-component plasma [32] and for a few state points of the Lennard-Jones fluid [33] show a similar level of agreement (if not better) with simulation data as RHNC results.

In this paper we will develop this idea, the reference functional approach, in more detail, generalizing the method to an arbitrary inhomogeneous situation and also analysing bulk fluid and wall–fluid correlations using the mixture description. We will see that, by introducing the reference functional, insertion free energies (i.e., the chemical potential in the bulk) are obtained quite naturally. For the wall–fluid problem treated in the bulk mixture approach this implies that the insertion free energy of the wall is explicitly given; using it we can show that in the case of a hard wall complete drying is predicted.

The paper is structured as follows: in section 2 we consider a fluid mixture in an arbitrary inhomogeneous equilibrium state and derive a general closure for the corresponding integral equations using the concept of the reference functional. This permits us to derive expressions for the insertion free energies corresponding to the change in grand potential when inserting the mixture particles into the inhomogeneous equilibrium state. In section 3 we apply the approach to a mixture of a Lennard-Jones fluid and hard particles. In the limit of infinite radius of the hard particles (upon which the particles become hard walls) and infinitely small hard-particle density we solve the equations for the fluid and wall–fluid correlation functions. For the bulk fluid, we find very good agreement with simulation for both the virial and internal energy equation of state. The liquid–vapour coexistence curve is obtained by (i) the usual Maxwell

construction and (ii) the requirement of complete drying at the hard wall. We discuss the form of the wall–fluid bridge function required to account for complete drying. Furthermore, we consider the consistency of our theory by analysing two sum rules appropriate to the density distributions at a hard wall. We discuss the relation of the reference functional method to commonly used density functional mean-field models. Section 4 contains a summary and perspectives for further research.

2. Theory

We consider a liquid mixture which contains n components. The interaction potential between atoms of species i and j is given by $u^{ij}(r)$ with $r = |\mathbf{r}_i - \mathbf{r}_j|$ denoting the distance between the two atoms ($i, j = 1, \ldots, n$). The ith element of the vector $\boldsymbol{\rho}(\mathbf{r}) = \{\rho_1(\mathbf{r}), \ldots, \rho_n(\mathbf{r})\}$ describes the density distribution of species i and likewise the ith element of the vector $\mathbf{V}(\mathbf{r}) = \{V_1(\mathbf{r}), \ldots, V_n(\mathbf{r})\}$ denotes the external potential acting on an atom of species i. In equilibrium, there exists a unique correspondence between the external potential $\mathbf{V}(\mathbf{r})$ and the density distribution which we denote by $\boldsymbol{\rho}_\mathbf{V}$ to highlight this correspondence. As a consequence, there exists a unique free-energy functional [34]

$$\mathcal{F}[\boldsymbol{\rho}] = \mathcal{F}^{\mathrm{id}}[\boldsymbol{\rho}] + \mathcal{F}^{\mathrm{ex}}[\boldsymbol{\rho}] \tag{1}$$

$$\beta\mathcal{F}^{\mathrm{id}}[\boldsymbol{\rho}] = \sum_i \int \mathrm{d}\mathbf{r}\, \rho_i(\mathbf{r}) \left(\log(\rho_i(\mathbf{r})\Lambda_i^3) - 1\right) \tag{2}$$

which is usually split into the exactly known ideal part (containing the species-specific de Broglie wavelength Λ_i) and the excess contribution. The grand free energy functional is defined by

$$\Omega[\boldsymbol{\rho}] = \mathcal{F}[\boldsymbol{\rho}] - \int \mathrm{d}\mathbf{r}\, (\boldsymbol{\mu}^{\mathrm{id}}(\rho_{i,0}) + \boldsymbol{\mu}^{\mathrm{ex}}(\rho_{i,0}) - \mathbf{V}(\mathbf{r})) \cdot \boldsymbol{\rho}(\mathbf{r}) \tag{3}$$

with $\boldsymbol{\mu}^{\mathrm{id}}(\rho_{i,0})$ denoting the chemical potential for an ideal mixture and $\boldsymbol{\mu}^{\mathrm{ex}}(\rho_{i,0})$ its excess (over ideal) for the asymptotic densities $\boldsymbol{\rho}_0 = \{\rho_{1,0}, \ldots, \rho_{n,0}\}$. The asymptotic densities correspond to the homogeneous density distribution for $\mathbf{V} = 0$. The components of the ideal chemical potential are given by $\beta\mu_i^{\mathrm{id}} = \log(\rho_{i,0}\Lambda_i^3)$ and $\beta = 1/(k_\mathrm{B}T)$ is the inverse temperature with Boltzmann's constant k_B. The equilibrium density distribution follows from

$$\left.\frac{\delta\Omega}{\delta\boldsymbol{\rho}(\mathbf{r})}\right|_{\rho=\rho_\mathbf{V}} = 0. \tag{4}$$

The free energy functional generates the hierarchy of (inhomogeneous) direct correlation functions by

$$\left.\beta\frac{\delta^n\mathcal{F}^{\mathrm{ex}}}{\delta\rho_{i_1}(\mathbf{r}_1)\cdots\delta\rho_{i_n}(\mathbf{r}_n)}\right|_{\rho=\rho_\mathbf{V}} = -c^{(n),i_1\cdots i_n}(\mathbf{r}_1, \ldots, \mathbf{r}_n; \boldsymbol{\rho}_\mathbf{V}). \tag{5}$$

The first member of the hierarchy is determined through equation (4):

$$c^{(1),i}(\mathbf{r}; \boldsymbol{\rho}_\mathbf{V}) = \log\frac{\rho_{\mathbf{V},i}(\mathbf{r})}{\rho_{0,i}} - \beta\mu_i^{\mathrm{ex}}(\boldsymbol{\rho}_0) + \beta V_i(\mathbf{r}). \tag{6}$$

We are now interested in the change of the density distribution $\boldsymbol{\rho}_\mathbf{V}$ generated through a perturbation corresponding to the external potential $\mathbf{V}' = \mathbf{V} + \Delta\mathbf{V}$. To this end we perform a functional Taylor expansion of the unknown excess free energy in the function variable $\Delta\boldsymbol{\rho}(\mathbf{r}) = \boldsymbol{\rho}(\mathbf{r}) - \boldsymbol{\rho}_\mathbf{V}(\mathbf{r})$ and define

$$\mathcal{F}^{\mathrm{ex}} = \mathcal{F}^{\mathrm{HNC}} + \mathcal{F}^{\mathrm{B}}. \tag{7}$$

Here, $\mathcal{F}^{\mathrm{HNC}}$ (the meaning of the label will become clear shortly) contains terms up to second order in $\Delta\boldsymbol{\rho}$ and all terms beyond second order are subsumed in $\mathcal{F}^{\mathrm{B}}$. By virtue of definition (5),

$$\beta\mathcal{F}^{\mathrm{HNC}} = \beta A^{\mathrm{ex}}(\boldsymbol{\rho}_{\mathbf{V}}) - \sum_i \int \mathrm{d}\mathbf{r}\, c^{(1),i}(\mathbf{r};\boldsymbol{\rho}_{\mathbf{V}})\Delta\rho_i(\mathbf{r}) - \tfrac{1}{2}\sum_{ij}\int \mathrm{d}\mathbf{r}\,\mathrm{d}\mathbf{r}'\, c^{(2),ij}(\mathbf{r},\mathbf{r}';\boldsymbol{\rho}_{\mathbf{V}})\Delta\rho_i(\mathbf{r})\Delta\rho_j(\mathbf{r}'), \tag{8}$$

where $A^{\mathrm{ex}}(\boldsymbol{\rho}_{\mathbf{V}})$ is the excess free energy of the equilibrium state corresponding to the external potential $\mathbf{V}$. Then the perturbed density distribution $\boldsymbol{\rho}_{\mathbf{V}'}$ corresponding to the external potential $\mathbf{V} + \Delta\mathbf{V}$ is according to equations (4) and (6)

$$\log\frac{\rho_{\mathbf{V}',i}(\mathbf{r})}{\rho_{\mathbf{V},i}(\mathbf{r})} + \beta\Delta V_i = \sum_k \int \mathrm{d}\mathbf{r}'\, c^{(2),ik}(\mathbf{r},\mathbf{r}';\boldsymbol{\rho}_{\mathbf{V}})\Delta\rho_k(\mathbf{r}') - \beta\frac{\delta\mathcal{F}^{\mathrm{B}}}{\delta\rho_i(\mathbf{r})}\bigg|_{\rho=\rho_{\mathbf{V}'}}. \tag{9}$$

It may appear that we have not gained very much from this formal manipulation: the density profile $\boldsymbol{\rho}_{\mathbf{V}'}$ is just expressed through the unknown density profile $\boldsymbol{\rho}_{\mathbf{V}}$, the corresponding unknown inhomogeneous direct correlation function $c^{(2),ij}(\mathbf{r},\mathbf{r}';\boldsymbol{\rho}_{\mathbf{V}})$ and the unknown functional $\mathcal{F}^{\mathrm{B}}$. Therefore we go to the *test particle limit*, i.e. we define the perturbation to $\mathbf{V}$ by fixing one atom of species j at position $\mathbf{r}_0$, thus $\Delta V_i(\mathbf{r}) = u^{ij}(\mathbf{r}-\mathbf{r}_0)$. For this particular choice of the perturbing potential, the density profiles are connected to the inhomogeneous pair correlation functions g^{ij} and $h^{ij} = g^{ij} - 1$ through

$$\rho_{\mathbf{V}',i}(\mathbf{r})\big|_{V_i'(\mathbf{r})=V_i(\mathbf{r})+u^{ij}(\mathbf{r}-\mathbf{r}_0)} = \rho_{\mathbf{V},i}(\mathbf{r})g^{ij}(\mathbf{r},\mathbf{r}_0;\boldsymbol{\rho}_{\mathbf{V}}), \tag{10}$$

$$\Delta\rho_{\mathbf{V}',i}(\mathbf{r})\big|_{V_i'(\mathbf{r})=V_i(\mathbf{r})+u^{ij}(\mathbf{r}-\mathbf{r}_0)} = \rho_{\mathbf{V},i}(\mathbf{r})h^{ij}(\mathbf{r},\mathbf{r}_0;\boldsymbol{\rho}_{\mathbf{V}}). \tag{11}$$

The inhomogeneous pair correlation functions are linked to the direct correlation functions via the inhomogeneous Ornstein–Zernike relation

$$h^{ij}(\mathbf{r},\mathbf{r}_0;\boldsymbol{\rho}_{\mathbf{V}}) - c^{(2),ij}(\mathbf{r},\mathbf{r}_0;\boldsymbol{\rho}_{\mathbf{V}}) = \sum_k \int \mathrm{d}\mathbf{r}'\,\rho_{\mathbf{V},k}(\mathbf{r}')c^{(2),ik}(\mathbf{r},\mathbf{r}';\boldsymbol{\rho}_{\mathbf{V}})h^{kj}(\mathbf{r}',\mathbf{r}_0;\boldsymbol{\rho}_{\mathbf{V}}). \tag{12}$$

Inserting equations (10)–(12) into (9) we recover the general closure relation for the inhomogeneous correlation functions

$$\log g^{ij}(\mathbf{r},\mathbf{r}_0;\boldsymbol{\rho}_{\mathbf{V}}) + \beta u^{ij}(\mathbf{r}-\mathbf{r}_0) = h^{ij}(\mathbf{r},\mathbf{r}_0;\boldsymbol{\rho}_{\mathbf{V}}) - c^{(2),ij}(\mathbf{r},\mathbf{r}_0;\boldsymbol{\rho}_{\mathbf{V}}) - \beta\frac{\delta\mathcal{F}^{\mathrm{B}}}{\delta\rho_i(\mathbf{r})}\bigg|_{\rho_i=\rho_{\mathbf{V},i}g^{ij}}, \tag{13}$$

which permits us to identify the density derivative of $\mathcal{F}^{\mathrm{B}}$ with the inhomogeneous bridge function:

$$b^{ij}(\mathbf{r},\mathbf{r}_0;\boldsymbol{\rho}_{\mathbf{V}}) = \beta\,\frac{\delta\mathcal{F}^{\mathrm{B}}}{\delta\rho_i(\mathbf{r})}\bigg|_{\rho_i(\mathbf{r})=\rho_{\mathbf{V},i}(\mathbf{r})g^{ij}(\mathbf{r},\mathbf{r}_0;\boldsymbol{\rho}_{\mathbf{V}})}. \tag{14}$$

So far all is exact, and at this point we recognize that upon setting $\mathcal{F}^{\mathrm{B}} = 0$ we recover the inhomogeneous HNC equations. Thus the HNC equations are generated by the second-order functional for the excess free energy, $\mathcal{F}^{\mathrm{HNC}}$, *in the test particle limit*. All higher orders in the density expansion of $\mathcal{F}^{\mathrm{ex}}$ contribute to the bridge function.

The unknown density profile $\boldsymbol{\rho}_{\mathbf{V}}(\mathbf{r})$ is connected to the correlation functions through the exact YBG equations:

$$\nabla\log\rho_{\mathbf{V},i}(\mathbf{r}) = \beta\nabla V_i(\mathbf{r}) + \beta\sum_j\int \mathrm{d}\mathbf{r}'\,h^{ij}(\mathbf{r},\mathbf{r}';\boldsymbol{\rho}_{\mathbf{V}})\rho_{\mathbf{V},j}(\mathbf{r}')\nabla V_j(\mathbf{r}'). \tag{15}$$

Using the inhomogeneous Ornstein–Zernike relation, equation (12), the last equation can be transformed into one connecting $\rho_{\mathbf{V},i}$ and $c^{(2),ij}$:

$$\nabla \log \rho_{\mathbf{V},i}(\mathbf{r}) = \beta \nabla V_i(\mathbf{r}) + \sum_j \int \mathrm{d}\mathbf{r}'\, c^{(2),ij}(\mathbf{r},\mathbf{r}';\boldsymbol{\rho}_\mathbf{V}) \nabla \rho_{\mathbf{V},j}(\mathbf{r}'). \tag{16}$$

Alternatively, this equation follows directly by taking the gradient in equation (6). Thus we see that upon specification of a suitable model for $\mathcal{F}^\mathrm{B}$, we have a closed system of equations for h^{ij}, $c^{(2),ij}$ and $\rho_{\mathbf{V},i}$ consisting of equations (12), (13), and (15) or (12), (13), and (16). This set of equations is standard in the theory of classical liquids and is usually derived using diagrammatic expansions [2] or functional methods [3]. The alternative derivation presented here provides the foundation for the derivation of insertion free energies which follows next.

The excess free energy pertaining to the external potential $\mathbf{V}$, $A^\mathrm{ex}(\boldsymbol{\rho}_\mathbf{V})$, and the corresponding one-body direct correlation function $c^{(1),i}(\mathbf{r};\boldsymbol{\rho}_\mathbf{V})$ do not appear in this system of equations. The latter can be determined using the potential distribution theorem [35] which states that $-c^{(1),i}/\beta$ is equivalent to the insertion free energy, i.e. the chemical potential, of a particle of species i into the inhomogeneous system defined by $\mathbf{V}$. By definition, this insertion free energy is the difference in grand potential with the test particle fixed at $\mathbf{r}_0$, say, and the grand potential without the test particle:

$$\beta\mu_i^\mathrm{ex}(\mathbf{r}_0;\boldsymbol{\rho}_\mathbf{V}) \equiv \beta\, \Omega[\boldsymbol{\rho}]|_{\boldsymbol{\rho}=\boldsymbol{\rho}_{\mathbf{V}'}} - \beta\, \Omega[\boldsymbol{\rho}]|_{\boldsymbol{\rho}=\boldsymbol{\rho}_\mathbf{V}} = -c^{(1),i}(\mathbf{r}_0;\boldsymbol{\rho}_\mathbf{V}) \tag{17}$$

where $V_j'(\mathbf{r}) = V_j(\mathbf{r}) + u^{ji}(\mathbf{r}-\mathbf{r}_0)$. Explicit evaluation yields (using the definition of Ω, equation (3), the expressions for the excess free energy, equations (7) and (8), and the definitions for the inhomogeneous correlation functions in equations (10) and (11))

$$\begin{aligned}
-c^{(1),i}(\mathbf{r}_0) = {} & \sum_j \int \mathrm{d}\mathbf{r}\, \rho_{\mathbf{V},j}(\mathbf{r}) g^{ji}(\mathbf{r},\mathbf{r}_0) \left(\log g^{ji}(\mathbf{r},\mathbf{r}_0) + \beta u^{ji}(\mathbf{r}-\mathbf{r}_0)\right) \\
& - \tfrac{1}{2} \sum_{jk} \int \mathrm{d}\mathbf{r} \int \mathrm{d}\mathbf{r}'\, \rho_{\mathbf{V},j}(\mathbf{r}) \rho_{\mathbf{V},k}(\mathbf{r}')\, c^{(2),jk}(\mathbf{r},\mathbf{r}') h^{ji}(\mathbf{r},\mathbf{r}_0) h^{ki}(\mathbf{r}',\mathbf{r}_0) \\
& - \sum_j \int \mathrm{d}\mathbf{r}\, \rho_{\mathbf{V},j}(\mathbf{r}) h^{ji}(\mathbf{r},\mathbf{r}_0) + \beta\, \mathcal{F}^\mathrm{B}[\boldsymbol{\rho}]\big|_{\rho_j(\mathbf{r})=\rho_{\mathbf{V},j} g^{ji}(\mathbf{r},\mathbf{r}_0)} .
\end{aligned} \tag{18}$$

For compactness, we have suppressed the variable '$\boldsymbol{\rho}_\mathbf{V}$' in all correlation functions which indicates that these pertain to the inhomogeneous density distribution defined by $\mathbf{V}$. We note that in deriving the last equation, A^ex has dropped out. To simplify this expression, we use the general closure relation (13), the inhomogeneous Ornstein–Zernike equation (12) and the definition (14):

$$-c^{(1),i}(\mathbf{r}_0) = -c^{(1),i}_\mathrm{HNC}(\mathbf{r}_0) - \sum_j \int \mathrm{d}\mathbf{r}\, \rho_{\mathbf{V},j}(\mathbf{r}) g^{ji}(\mathbf{r},\mathbf{r}_0) b^{ji}(\mathbf{r},\mathbf{r}_0) + \beta\, \mathcal{F}^\mathrm{B}[\boldsymbol{\rho}]\big|_{\rho_j(\mathbf{r})=\rho_{\mathbf{V},j} g^{ji}(\mathbf{r},\mathbf{r}_0)} . \tag{19}$$

This new result, which is the main formal result of our paper, constitutes the generalization of the well known HNC result for the chemical potential in inhomogeneous systems[1] to closures with non-vanishing bridge functions. Here, $-c^{(1),i}_\mathrm{HNC}(\mathbf{r}_0)/\beta$ describes the position-dependent HNC insertion free energy for $\mathcal{F}^\mathrm{B} = 0$:

$$-c^{(1),i}_\mathrm{HNC}(\mathbf{r}_0) = \sum_j \int \mathrm{d}\mathbf{r}\, \rho_{\mathbf{V},j}(\mathbf{r}) \left(\tfrac{1}{2} h^{ji}(\mathbf{r},\mathbf{r}_0) \left[h^{ji}(\mathbf{r},\mathbf{r}_0) - c^{(2),ji}(\mathbf{r},\mathbf{r}_0)\right] - c^{(2),ji}(\mathbf{r},\mathbf{r}_0)\right) . \tag{20}$$

[1] See [13] for a derivation using the well known charging method.

Note that $c^{(1),i}$ is determined by the density distribution $\boldsymbol{\rho}_{\mathbf{V}}$ through equation (6) which imposes a consistency constraint on all subsequent approximations to $\mathcal{F}^{\mathrm{B}}$. Considering the limit $|\mathbf{r}_0| \to \infty$, we may assume that the external potential vanishes, $\mathbf{V}(\mathbf{r}_0) \to 0$, thus $\boldsymbol{\rho}_{\mathbf{V}} \to \boldsymbol{\rho}_0$ and the inhomogeneous correlation functions become the bulk correlation functions, $g^{ji}(\mathbf{r}, \mathbf{r}_0) \to g^{ji}(\mathbf{r} - \mathbf{r}_0)$. Then equations (6) and (19) imply an equation for the excess chemical potential of species i *in the bulk*:

$$\beta\mu_i^{\mathrm{ex}}(\boldsymbol{\rho}_0) = \beta\mu_i^{\mathrm{ex,HNC}}(\boldsymbol{\rho}_0) - \sum_j \rho_{0,j} \int \mathrm{d}\mathbf{r}\, g^{ji}(\mathbf{r}) b^{ji}(\mathbf{r}) + \beta\, \mathcal{F}^{\mathrm{B}}[\boldsymbol{\rho}]\big|_{\rho_j(\mathbf{r})=\rho_{0,j} g^{ji}(\mathbf{r})}, \tag{21}$$

$$\beta\mu_i^{\mathrm{ex,HNC}}(\boldsymbol{\rho}_0) = \sum_j \rho_{0,j} \int \mathrm{d}\mathbf{r}\, (\tfrac{1}{2} h^{ji}(\mathbf{r})[h^{ji}(\mathbf{r}) - c^{(2),ji}(\mathbf{r})] - c^{(2),ji}(\mathbf{r})). \tag{22}$$

The same equation is derived if $\mathbf{V} = 0$ is assumed from the outset, i.e. if the functional expansion of the excess free energy is performed around the bulk state described by $\boldsymbol{\rho}_0$.

In general, the excess free energy functional beyond second order, the bridge functional $\mathcal{F}^{\mathrm{B}}$, is not known. However, we may approximate $\mathcal{F}^{\mathrm{B}}$ by a density functional for a reference system in the following manner:

$$\mathcal{F}^{\mathrm{B}}[\boldsymbol{\rho}] \approx \mathcal{F}^{\mathrm{B,ref}}[\boldsymbol{\rho}] = \mathcal{F}^{\mathrm{ref}}[\boldsymbol{\rho}] - \mathcal{F}^{\mathrm{HNC,ref}}[\boldsymbol{\rho}], \tag{23}$$

where the second-order HNC contribution is given by equation (8):

$$\begin{aligned}\beta\mathcal{F}^{\mathrm{HNC,ref}}[\boldsymbol{\rho}] = \beta A^{\mathrm{ex,ref}}(\boldsymbol{\rho}_{\mathbf{V}}) &- \sum_i \int \mathrm{d}\mathbf{r}\, c_{\mathrm{ref}}^{(1),i}(\mathbf{r};\boldsymbol{\rho}_{\mathbf{V}})\Delta\rho_i(\mathbf{r}) \\ &- \tfrac{1}{2}\sum_{ij} \int \mathrm{d}\mathbf{r}\,\mathrm{d}\mathbf{r}'\, c_{\mathrm{ref}}^{(2),ij}(\mathbf{r},\mathbf{r}';\boldsymbol{\rho}_{\mathbf{V}})\Delta\rho_i(\mathbf{r})\Delta\rho_j(\mathbf{r}').\end{aligned} \tag{24}$$

For an explicitly given functional $\mathcal{F}^{\mathrm{ref}}$, the direct correlation functions $c_{\mathrm{ref}}^{(1),i}$ and $c_{\mathrm{ref}}^{(2),ij}$ are obtained through equation (5). The reference functional approximation implies that all direct correlations beyond second order are well approximated by the corresponding direct correlations of the reference system. Equivalently, it states that the contributions to the excess free energy beyond those of the reference system are of second order in the density difference $\Delta\boldsymbol{\rho}$,

$$\Delta A = \mathcal{F}^{\mathrm{ex}}[\boldsymbol{\rho}] - \mathcal{F}^{\mathrm{ex,ref}}[\boldsymbol{\rho}] = \mathcal{F}^{\mathrm{HNC}}[\boldsymbol{\rho}] - \mathcal{F}^{\mathrm{HNC,ref}}[\boldsymbol{\rho}] \tag{25}$$

$$\begin{aligned}&= \mathrm{const} - \frac{1}{\beta}\sum_i \int \mathrm{d}\mathbf{r}\, (c^{(1),i} - c_{\mathrm{ref}}^{(1),i})(\mathbf{r};\boldsymbol{\rho}_{\mathbf{V}})\Delta\rho_i(\mathbf{r}) \\ &\quad - \frac{1}{2\beta}\sum_{ij} \int \mathrm{d}\mathbf{r}\,\mathrm{d}\mathbf{r}'\, (c^{(2),ij} - c_{\mathrm{ref}}^{(2),ij})(\mathbf{r},\mathbf{r}';\boldsymbol{\rho}_{\mathbf{V}})\Delta\rho_i(\mathbf{r})\Delta\rho_j(\mathbf{r}').\end{aligned} \tag{26}$$

Thus the reference functional approximation defines a kind of a generalized mean-field approximation in treating a general fluid beyond a given reference system where the coefficient in the quadratic term, $c^{(2),ij} - c_{\mathrm{ref}}^{(2),ij}$, is determined self-consistently.

In practice, there are only three reference systems for which we possess reasonably accurate density functionals. They are all related to hard-sphere systems where we can use geometric arguments for their construction. These encompass (i) functionals of Rosenfeld type for hard-sphere mixtures (see e.g. [25, 26]), (ii) a functional for the Asakura–Oosawa colloid–polymer mixture [36], and (iii) a recently proposed functional for non-additive hard-sphere mixtures [37]. The functionals of type (i) have been tested in a variety of inhomogeneous situations and can be regarded as very robust. Functional (ii) has been applied to the structure of free interfaces and near a hard wall, predicting a wealth of interesting phenomena [36].

A drawback is that the polymers are treated only linearly in their density, consequently correlations from the functional are deficient if they are sensitive to higher orders in the polymer density. Functional (iii) has not been tested yet for inhomogeneous situations. It contains the functional for the Asakura–Oosawa model as a limiting case, so similar merits and problems may be expected there.

These reference functionals contain a number of parameters (hard-sphere diameters, non-additivity parameters, ...) that have to be fixed in a practical application. For expansions around bulk densities one may exploit the similarity to the reference HNC and use Lado's criterion [31, 38]. Another criterion is proposed in equation (36) below. However, the unique fixing of the reference system, especially for the inhomogeneous case, remains to be studied in the future.

Summarizing the literature which is concerned with the reference functional idea, we note that the formalism presented above has been formulated previously only for functionals of type (i) and for functional expansions around bulk densities ρ_0, i.e. $\mathbf{V} = 0$. In fact, the reference functional approximation as expressed by equation (23) was introduced in [31] and used to describe the one-component plasma with high accuracy and its similarity to the reference HNC equations was also pointed out. Later on, the numerical efficacy of this idea was illustrated for a few state points of the one-component Lennard-Jones (LJ) fluid [33] and of binary mixtures with their size asymmetry being not too large [38]. Comparison with simulation results for both the correlation functions and thermodynamic properties shows very good agreement.

Although the hard-sphere functionals of type (i) are very robust, they are not exact. For example, the bulk direct correlation function obtained from the functionals by direct functional differentiation, equation (5), represent good approximations for its behaviour inside the hard core but predict it to be zero outside. In order to improve upon the accuracy of the correlation functions, the reference functional method may be applied to the hard-sphere reference system itself. As a result, for one-component hard spheres the bridge function for the bulk integral equations generated by using the White Bear functional of [26] appears to be the most accurate one known up to now. Applied to binary hard-sphere mixtures and size asymmetries >10, the bulk integral equation closure shows deficiencies in calculating the distribution function between the big spheres [39]. This may be related to the inadequacy of the functional Taylor expansion around *bulk* densities for large size asymmetries or to the inadequacy of the functionals themselves (as manifest in a low-density analysis of the third-order direct correlation function $c^{(3)}$ [40]).

The advantage of the present formalism is that for a general, inhomogeneous density distribution $\boldsymbol{\rho}_{\mathbf{V}}$ it is possible to determine directly insertion free energies using equation (19). Of much interest is e.g. obtaining the insertion free energy for colloids at fluid interfaces which determines their adsorption behaviour at the interface. However, a numerical solution of equations (12)–(15) requires large numerical efforts. Functional minimization in two or three dimensions is complicated by the nature of the three types of functionals mentioned above; these contain δ and θ-like distributions.

As outlined at the end of section 1 we confine ourselves in the following to an illustration of the approach for a simple one-component fluid (in the bulk and near a hard wall) and for $\mathbf{V} = 0$.

3. Application: equation of state for a simple fluid and drying at a hard wall

We consider a binary mixture of cut-off and shifted Lennard-Jones particles (species 1) with hard cavities of radius R_c (species 2). Let

$$u_{\mathrm{LJ}}(r) = 4\epsilon \left[(r/\sigma)^{-6} - (r/\sigma)^{-12} \right] \tag{27}$$

then the interaction potentials in the mixture are given by

$$u^{11}(r) = \begin{cases} u_{\mathrm{LJ}}(r) - u_{\mathrm{LJ}}(r_{\mathrm{c}}) & (r \leqslant r_{\mathrm{c}}) \\ 0 & (r > r_{\mathrm{c}}), \end{cases} \tag{28}$$

$$\exp(-\beta u^{12}(r)) = \exp(-\beta u^{21}(r)) = \theta(R_{\mathrm{c}} - r), \tag{29}$$

$$\exp(-\beta u^{22}(r)) = \theta(2R_{\mathrm{c}} - r). \tag{30}$$

We apply the formalism from the last chapter with $\boldsymbol{\rho}_{\mathbf{V}} = \{\rho_{1,0}, \rho_{2,0}\}$ and for the reference system we use the original Rosenfeld functional [25] (defined in appendix A) which contains two unknown hard-sphere diameters d_1 and d_2. In the limit $\rho_{2,0} \to 0$ ($\rho_{1,0} \equiv \rho_0$) the equations for $h^{11} \equiv h$ and $c^{(2),11} \equiv c^{(2)}$ (fluid correlations) and h^{12} (cavity–fluid correlation) decouple. The integral equation system for the LJ fluid (see equations (12) and (13)) is given by

$$\log g(\mathbf{r}) + \beta u^{11}(\mathbf{r}) = h(\mathbf{r}) - c^{(2)}(\mathbf{r}) - \beta \frac{\delta \mathcal{F}^{\mathrm{B,ref}}}{\delta \rho(\mathbf{r})}\bigg|_{\rho(\mathbf{r})=\rho_0 g(\mathbf{r})}, \tag{31}$$

$$h(\mathbf{r}) - c^{(2)}(\mathbf{r}) = \rho_0 h * c^{(2)}(\mathbf{r}) \tag{32}$$

$$\left(h * c^{(2)}(\mathbf{r}) = \int \mathrm{d}\mathbf{r}'\, c^{(2)}(\mathbf{r} - \mathbf{r}') h(\mathbf{r}') \right), \tag{33}$$

with $g(\mathbf{r}) \equiv g(r)$ etc. Following the reference functional assumption, $\mathcal{F}^{\mathrm{B}}$ has been replaced by the corresponding functional for the reference system, see equation (23), and the fluid bridge function is given by

$$b(\mathbf{r}) = \beta \frac{\delta \mathcal{F}^{\mathrm{B,ref}}}{\delta \rho(\mathbf{r})}\bigg|_{\rho(\mathbf{r})=\rho_0 g(\mathbf{r})}. \tag{34}$$

Using the Ornstein–Zernike equation in the limit $\rho_{2,0} \to 0$ in equation (13) yields a single equation for the cavity–particle correlation which, however, needs as input the solution for $c^{(2)}$, the pair direct fluid correlation function:

$$\log g^{12}(\mathbf{r}) + \beta u^{12}(\mathbf{r}) = \rho_0 h^{12} * c^{(2)}(\mathbf{r}) - \beta \frac{\delta \mathcal{F}^{\mathrm{B,ref}}}{\delta \rho(\mathbf{r})}\bigg|_{\rho(\mathbf{r})=\rho_0 g^{12}(\mathbf{r})}. \tag{35}$$

In taking the planar hard-wall limit $R_{\mathrm{c}} \to \infty$, we shift the origin of the coordinate system such that $\lim_{R_{\mathrm{c}}\to\infty} \exp(-\beta u^{12}(\mathbf{r})) = \theta(z)$. In this limit, the cavity–fluid correlation functions will be referred to as the wall–fluid correlation functions.

Note that in the dilute limit $\rho_{2,0} \to 0$ both the system of equations (31), (32) and (35) can be derived directly from minimization of the grand potential employing the excess free energy functional *of the one-component LJ fluid*, $\mathcal{F}^{\mathrm{HNC}}[\rho(\mathbf{r})] + \mathcal{F}^{\mathrm{B,ref}}[\rho(\mathbf{r}); d_1]$, and using u^{11} and u^{12}, respectively, as external potentials. Consequently, the reference functional $\mathcal{F}^{\mathrm{B,ref}}$ is derived from the one-component Rosenfeld functional and contains only one unknown parameter, the hard-sphere diameter d_1.

Both equations (31) and (35) are similar to the reference HNC closure [8]. There, the bridge function is approximated directly by the bridge function of the reference system whereas here the bridge function is obtained from the reference system *free energy functional*. For state points near the triple point, both prescriptions agree with each other closely. However, in reference HNC the fluid bridge function remains short ranged near the bulk critical point as does the wall–fluid bridge function near coexistence on the liquid side. Thus reference HNC omits effects of bulk criticality and of drying at the hard wall. In the present scheme, the fluid bridge function becomes long ranged through its functional dependence on the fluid correlation function g (which is long ranged near the critical point) and so does the wall–fluid bridge function near coexistence through its dependence on the wall–particle correlation

function g^{12}. As will be seen, this does not lead to the correct bulk critical behaviour for the fluid but drying at the hard wall is described very well.

For the determination of the unknown hard-sphere diameter d_1 we propose the following criterion:

$$\frac{\partial}{\partial d_1}\left(\mathcal{F}^{\mathrm{B,ref}}[\rho_0 g(\mathbf{r}); d_1] - \mathcal{F}^{\mathrm{B,ref}}[\rho_0 g^{\mathrm{ref}}(\mathbf{r}); d_1]\right) \stackrel{!}{=} 0, \tag{36}$$

which corresponds to extremizing the free energy difference between the fluid and the reference system with respect to d_1. The correlation function of the reference system g^{ref} is taken to be the Percus–Yevick correlation function consistent with the Rosenfeld functional. This criterion is local in the bulk state space (ρ, T) and turns out to be practicable and reliable; furthermore, it is seen in the numerical results that in the moderate to high density region it is equivalent to the usual reference HNC criterion [8]. However, a deeper understanding of equation (36) with regard to a unique specification of the reference system is absent at this point.

For the numerical calculations, we use the cut-off $r_c = 4\sigma$ for which an extensive body of simulation data for the equation of state exists [41].

3.1. Equation of state

The pressure p and the excess (over ideal) internal energy per particle u are determined from the fluid pair correlation function through the well known equations

$$\frac{\beta p}{\rho_0} = 1 - \frac{2}{3}\pi\rho_0\beta\int_0^\infty \mathrm{d}r\, r^3 g(r)\frac{\mathrm{d}u^{11}(r)}{\mathrm{d}r}, \tag{37}$$

$$u = 2\pi\rho_0\int_0^\infty \mathrm{d}r\, r^2 g(r) u^{11}(r). \tag{38}$$

The usual consistency check of integral equation closures proceeds via the compressibility relation

$$\beta\frac{\partial p}{\partial\rho_0} = 1 - 4\pi\int_0^\infty \mathrm{d}r\, r^2 c^{(2)}(r). \tag{39}$$

In principle, the excess Helmholtz free energy per particle a^{ex} can be determined through integration of equation (38) along isochores,

$$\beta a^{\mathrm{ex}} = \int_0^\beta u(\beta')\,\mathrm{d}\beta', \tag{40}$$

and the excess chemical potential follows by differentiating on an isotherm

$$\mu^{\mathrm{ex}} = a^{\mathrm{ex}} + \rho_0\frac{\partial a^{\mathrm{ex}}}{\partial\rho_0}. \tag{41}$$

However, in the reference functional approach the excess chemical potential is given directly by (see equation (21))

$$\beta\mu^{\mathrm{ex}} = \beta\mu^{\mathrm{ex,HNC}} - 4\pi\rho_0\int_0^\infty \mathrm{d}r\, r^2 b(r) g(r) + \beta\mathcal{F}^{\mathrm{B,ref}}[\rho_0 g(r); d_1], \tag{42}$$

$$\beta\mu^{\mathrm{ex,HNC}} = 4\pi\rho_0\int_0^\infty \mathrm{d}r\, r^2\left(\tfrac{1}{2}h(r)\left[h(r) - c^{(2)}(r)\right] - c^{(2)}(r)\right). \tag{43}$$

Consistency with the virial equation (37) may be checked using the isothermal Gibbs–Duhem relation

$$\frac{\partial p}{\partial\mu} = \rho_0, \qquad (\mu = \mu^{\mathrm{id}} + \mu^{\mathrm{ex}}). \tag{44}$$

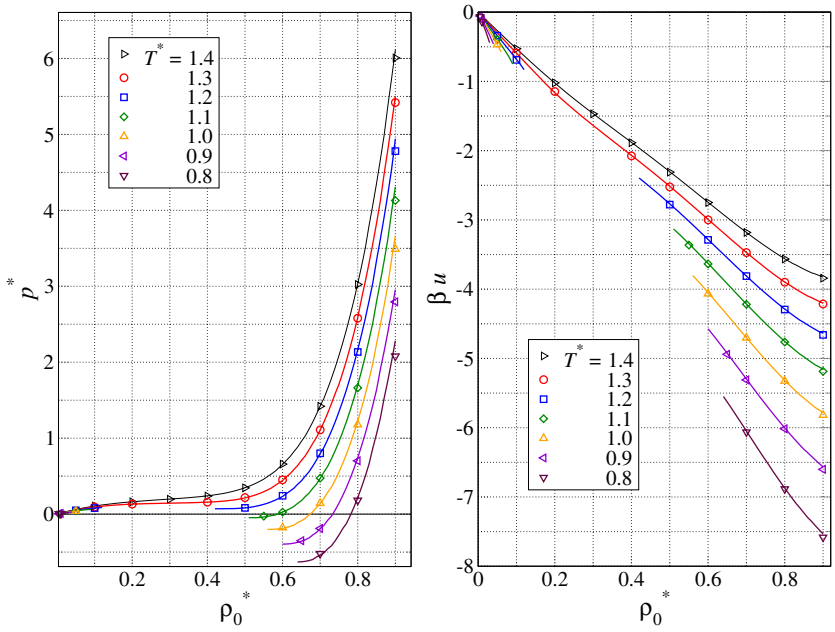

Figure 1. Left panel: virial equation of state at various temperatures, $p^* = p^*(\rho_0^*)$. The pressure is calculated according to equation (37). Right panel: internal energy equation of state at various temperatures, $\beta u = \beta u(\rho_0^*)$. The excess internal energy is calculated according to equation (38). The symbols denote simulation data taken from [41].

From the simulations of [41] the critical temperature and density of the cut-off and shifted LJ fluid can be estimated as $T_c^* \approx 1.25$ and $\rho_c^* \approx 0.31$.[2] In figure 1, we present our results for $p^*(\rho_0^*)$ and $\beta u(\rho_0^*)$ for temperatures $T^* = 0.8 \cdots 1.4$. We see that for all temperatures and densities (both close to and away from the critical region) the pressure and internal energy calculated from the reference functional match the simulation data very well. This indicates that the pair correlation function $g(r)$ is very accurate within the range of $u^{11}(r)$ (see equations (37) and (38)). In figure 2, we check the consistency of the virial and the compressibility equation of state (upper panel) and the Gibbs–Duhem relation (lower panel) with the chemical potential calculated via the insertion method, equation (42). Clearly, for the critical region, roughly delineated by $T^* = 1.2 \cdots 1.3$ and $\rho_0^* = 0.15 \cdots 0.5$, we observe inconsistencies between the virial and compressibility equation of state, and, somewhat weaker, deviations from $(\partial p/\partial \mu)/\rho_0 = 1$. However, outside the critical region and for stable bulk densities ρ_0, the ratio of $\partial p/\partial \rho_0$ calculated via equation (39) and via the derivative of equation (37) indicates violations of at most 20%, and the Gibbs–Duhem relation is satisfied rather well. This will be important for the subsequent investigation of drying at the hard wall.

3.2. Two routes to liquid–vapour coexistence and drying at the hard wall

Integral equations usually give results for pair correlation functions in the metastable as well as in the stable region, and therefore it is customary to obtain the coexistence curve by requiring $\mu(\rho_l) = \mu(\rho_g)$ and $p(\rho_l) = p(\rho_g)$; this is equivalent to employing a common tangent or

[2] Reduced units, denoted by an asterisk, are defined by setting $\epsilon = \sigma = k_B = 1$.

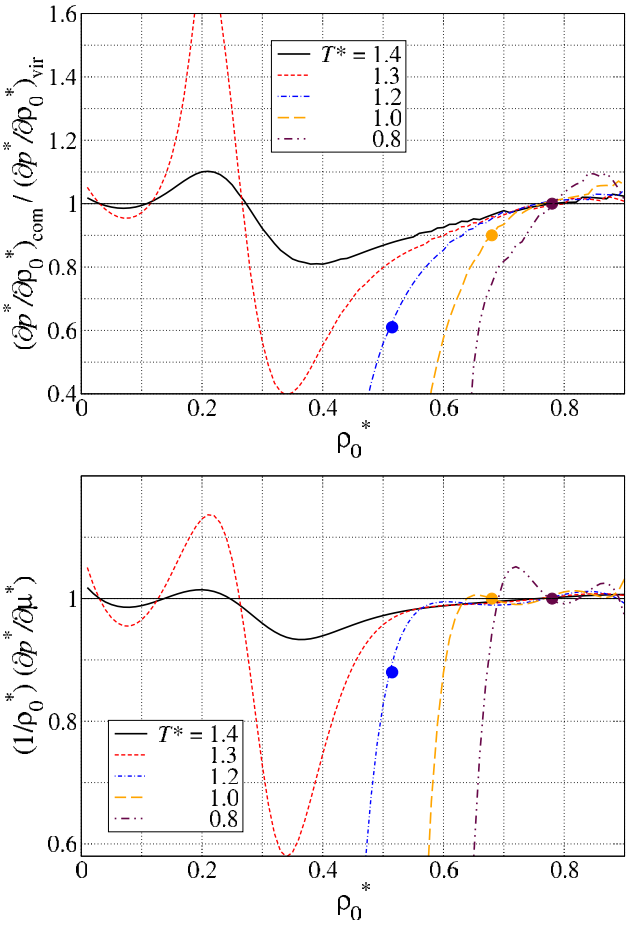

Figure 2. Testing the consistency of the equation of state at various temperatures. Upper panel: the ratio of the density derivatives of the pressure, calculated (i) using the compressibility equation (39) and (ii) via the derivative of a polynomial fit to the virial pressure, equation (37). Lower panel: the ratio of the chemical potential derivative of the virial pressure and the bulk density. In order to perform the derivative, both the virial pressure, equation (37), and the chemical potential, equation (42), were fitted to polynomials in the bulk density. In both panels, the density coordinate of the filled circles for the three lowest temperatures T^* indicates the corresponding coexistence density of the liquid phase obtained from simulations [41].

Maxwell construction. The density of the coexisting liquid is given by ρ_l, while ρ_g denotes the coexisting gas density. The pressure is given by equation (37) and the chemical potential may be calculated by either equation (41) or in our case equation (42).

However, one may avoid the problem of dealing with correlation functions in the metastable domain altogether if one defines ρ_l as the bulk density for which complete drying at a hard wall occurs at a given $T < T_c$. Correspondingly, ρ_g is then the density in the bulk of the infinitely extended drying film.

In order to understand the physics of drying [42], let us consider a liquid of density ρ_0 near a hard wall at fixed temperature which is close to coexistence, expressed by $\delta\mu = \mu(\rho_0) - \mu(\rho_l) > 0$ and $\delta\mu$ small. Since the wall exerts no attractive forces on the fluid molecules, we would expect the fluid density near the wall to be gaslike as this is energetically

more favourable. Corroborating this argument, there exists a sum rule relating the fluid density at the hard wall, ρ_c, to the bulk pressure of the liquid,

$$\begin{aligned}\rho_c &= \beta p(\mu(\rho)) \\ &\approx \beta(p(\mu(\rho_l)) + \rho_l \delta\mu), \\ &\approx \rho_g + \beta(\beta_1 \rho_g^2/2 + \rho_l \delta\mu),\end{aligned} \tag{45}$$

(see also equation (63) below). Since the second virial coefficient of a simple liquid, β_1, is negative, this sum rule tells us that $\rho_c < \rho_g$ for $\delta\mu \to 0$. Therefore the density profile must pass from a value smaller than the coexisting gas density at the wall to the liquid density in the bulk. Since we can safely assume (for $T < T_c$) that the transition from ρ_g to ρ_l happens within a few molecular diameters we are led to the hypothesis that upon $\delta\mu \to 0$ a gas layer forms between the hard wall and the bulk liquid whose width l goes to infinity as $\delta\mu \to 0$ *for all* $T < T_c$—complete drying occurs. More formally, the emergence of the gas film may be treated using a coarse-grained interface Hamiltonian which in mean-field approximation predicts a slow divergence of the gas film width upon approaching coexistence: $l \propto -\ln \delta\mu$. For a recent general analysis of liquids with short-ranged attractions near spherical hard walls, see [44].

We may obtain the coexisting densities in the hard-wall route without explicitly solving the wall–fluid integral equation by examining the stability of a solution with infinitely extended gas film. Having obtained these we checked explicitly that the adsorption obtained from the numerical solution to the wall–fluid equation diverges upon approaching the liquid coexisting density from above; examples are found in figures 4 (bottom panel) and 8 below. The grand potential functional which yields the wall–fluid equation is given by

$$\Omega[\rho] = \mathcal{F}^{\mathrm{id}}[\rho(\mathbf{r})] + \mathcal{F}^{\mathrm{HNC}}[\rho(\mathbf{r})] + \mathcal{F}^{\mathrm{B,ref}}[\rho(\mathbf{r})] - \int \mathrm{d}r\, (\mu(\rho_l) - u^{12}(\mathbf{r}))\rho(\mathbf{r}), \tag{46}$$

with $u^{12}(\mathbf{r}) \to u^{12}(z)$, the planar hard-wall potential. The excess free energy functional $\mathcal{F}^{\mathrm{HNC}} + \mathcal{F}^{\mathrm{B,ref}}$ is given by the Taylor expansion around the liquid bulk density $\rho_0 = \rho_l$. When examining the stability conditions of an infinitely extended drying film between the wall and the infinitely extended bulk liquid, we can neglect the hard-wall potential u^{12} and the grand potential functional in equation (46) simply becomes the bulk grand potential in a Taylor expansion around ρ_l. As a first condition, the grand potential of the drying film with density ρ_g must be stationary

$$\left.\frac{\delta\Omega}{\delta\rho(\mathbf{r})}\right|_{\rho(\mathbf{r})=\rho_g} \stackrel{!}{=} 0. \tag{47}$$

Let V denote the system volume. We introduce the bulk densities of the grand potential, $\omega(\rho) = \Omega(\rho)/V$, and of the free energy, $f(\rho) = \mathcal{F}(\rho)/V$. The second condition is that the drying film can only coexist with the liquid if the grand potential densities for the two bulk densities ρ_g and ρ_l are equal:

$$\omega(\rho_g) - \omega(\rho_l) \stackrel{!}{=} 0. \tag{48}$$

We insert the grand potential of equation (46) into the above two conditions, evaluate them at the required coexisting bulk densities and using the abbreviations $\Delta\mu = \mu(\rho_g) - \mu(\rho_l)$, $\Delta\omega = \omega(\rho_g) - \omega(\rho_l)$ we obtain

$$\begin{aligned}0 \stackrel{!}{=} \beta\Delta\mu = {} & \beta\mu^{\mathrm{ex,ref}}(\rho_g; d_{1,l}) - \beta\mu^{\mathrm{ex,ref}}(\rho_l; d_{1,l}) \\ & + \left[\tilde{c}^{(2)}(0; \rho_l) - \tilde{c}^{(2),\mathrm{ref}}(0; d_{1,l})\right](\rho_g - \rho_l) + \log\frac{\rho_l}{\rho_g},\end{aligned} \tag{49}$$

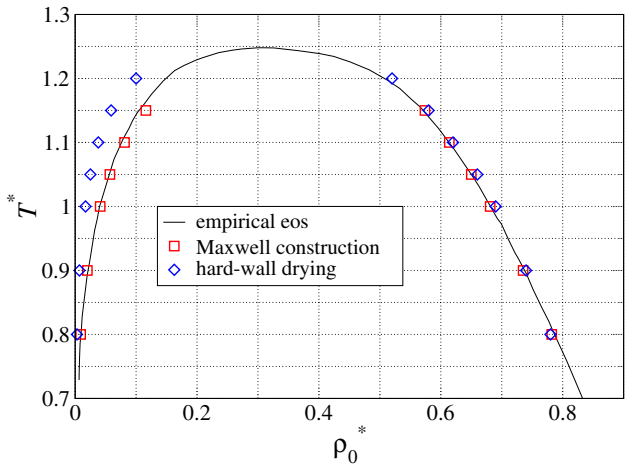

Figure 3. Liquid–gas coexistence for the cut-off and shifted LJ fluid. The curve is derived from an empirical fit to the free energy of the full LJ fluid, using mean-field corrections to account for the cut-off and shift in the potential [41]. The squares are the coexistence points derived by the Maxwell construction using equations (37) and (42). The diamonds are the coexistence points obtained by considering complete drying at the hard wall expressed through equations (49) and (50).

$$0 \stackrel{!}{=} \Delta\omega = f^{\mathrm{ex,ref}}(\rho_\mathrm{l}; d_{1,\mathrm{l}}) - f^{\mathrm{ex,ref}}(\rho_\mathrm{g}; d_{1,\mathrm{l}}) + \frac{1}{\beta}(\rho_\mathrm{l} - \rho_\mathrm{g}) - \left[\rho_\mathrm{l}\mu^{\mathrm{ex,ref}}(\rho_\mathrm{l}; d_{1,\mathrm{l}}) - \rho_\mathrm{g}\mu^{\mathrm{ex,ref}}(\rho_\mathrm{g}; d_{1,\mathrm{l}})\right] + \frac{1}{2\beta}\left[\tilde{c}^{(2)}(0; \rho_\mathrm{l}) - \tilde{c}^{(2),\mathrm{ref}}(0; d_{1,\mathrm{l}})\right](\rho_\mathrm{l}^2 - \rho_\mathrm{g}^2). \tag{50}$$

Here, $d_{1,\mathrm{l}} = d_1(\rho_\mathrm{l})$ is the reference hard-sphere diameter which is determined by condition (36) and $\tilde{c}^{(2)}(k)$ is the Fourier transform of $c^{(2)}(r)$. The system of equations (49) and (50) can be solved for ρ_l and ρ_g along with the simultaneous solution to the integral equations (31) and (32) for the liquid (which is needed to obtain $\tilde{c}^{(2)}(0; \rho_\mathrm{l})$).

In figure 3 we compare the coexistence curve from the standard Maxwell construction (using equations (37) and (42)) and that from hard-wall drying with a curve fitted to simulation data from [41] which was obtained from an equation of state. In agreement with our findings concerning the accuracy of the Gibbs–Duhem equation (see figure (2)), the Maxwell construction gives an excellent description of the coexistence curve away from the critical region. Closer to the critical point, we are not able to find a solution using the Maxwell construction. This can be traced back to the violation of the Gibbs–Duhem equation. Hard-wall drying yields coexisting liquid densities with similar accuracy but there are clear deviations from simulations for the coexisting gas densities are clearly visible. The reason for this lies in the error in extrapolating the bulk grand potential density, equation (50), to low densities, using only bulk properties of the reference system and the pair direct correlation function of the coexisting liquid state point. Nevertheless, the fair agreement between the results from the Maxwell construction and from hard-wall drying is most encouraging, and, to our knowledge, has not been achieved before within integral equation approaches.

Upon approaching the coexisting liquid density from above on an isotherm, the wall–liquid adsorption density Γ_wl diverges and the wall–liquid surface tension γ_wl approaches the sum of the liquid–gas surface tension $\gamma_\mathrm{gl}^\infty$ and the wall–gas surface tension γ_wg. A mean-field analysis of an effective interface Hamiltonian for this situation gives [44]

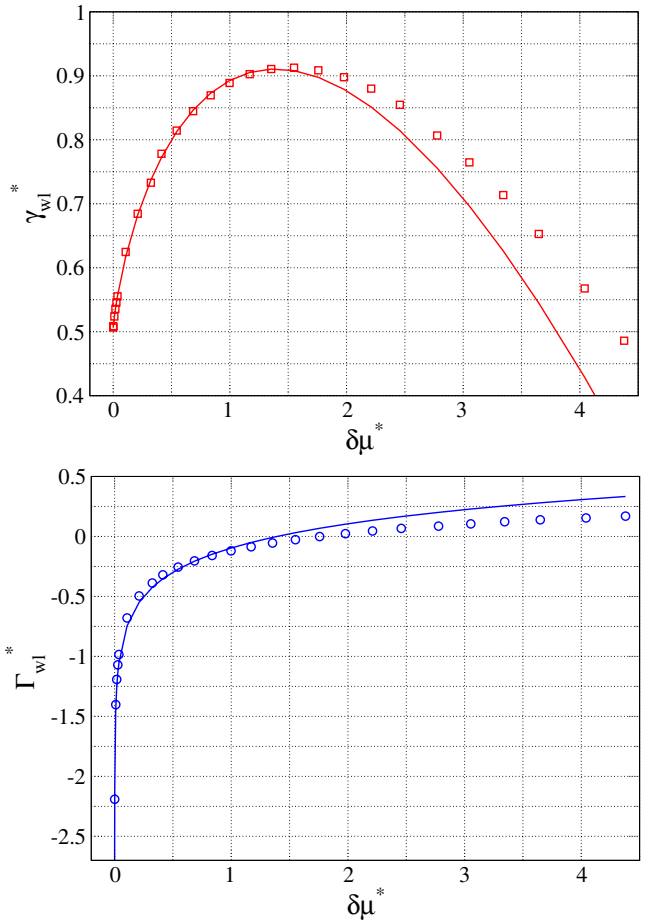

Figure 4. Surface tension (top panel) and adsorption density (bottom panel) of the cut-off and shifted LJ fluid at a hard wall at temperature $T^* = 1.0$. Symbols are integral equation results and curves correspond to a fit near coexistence to the functional form given in equations (51) and (52), setting $\gamma_{wg}(\mu)$ to a constant and neglecting $\Gamma_{wg}(\mu)$. From the fit we extract the bulk correlation length $\xi \approx 0.45\,\sigma$ and $a \approx 0.89\,k_B T/\sigma^3$. The range of the chemical potential covered by the integral equation results corresponds to the bulk densities $\rho_0^* = 0.686 \cdots 0.9$.

$$\gamma_{wl}(\mu) = \gamma_{wg}(\mu) + \gamma_{gl}^{\infty} + \xi\,\Delta\rho\,\delta\mu\left[\ln\left(\frac{a}{\Delta\rho\,\delta\mu}\right) + 1\right], \tag{51}$$

$$\Gamma_{wl}(\mu) = \Gamma_{wg}(\mu) - \xi\,\Delta\rho\,\ln\left(\frac{a}{\Delta\rho\,\delta\mu}\right). \tag{52}$$

Here, $\mu = \mu(\rho_0)$ is the chemical potential in the bulk, far away from the wall ($\delta\mu = \mu - \mu(\rho_l)$), $\Delta\rho = \rho_l - \rho_g$ is the difference of the coexisting densities, and ξ is the decay length of the correlation function in the gas phase. The effective parameter a is of order $O(k_B T/\xi^3)$. Fluctuations are expected to change the above behaviour only slightly; a treatment within the interface Hamiltonian approach [44] yields a renormalization of the bulk correlation length: $\xi \to (1 + \omega/2)\,\xi$ with $\omega = k_B T/(4\pi\,\gamma_{gl}^{\infty}\,\xi^2)$.

We have analysed the surface tension and the adsorption density for the isotherm $T^* = 1.0$. The adsorption density is given by

$$\Gamma_{\mathrm{wl}} = \rho_0 \int_0^\infty h^{12}(z)\,\mathrm{d}z, \tag{53}$$

while the surface tension γ_{wl} can be derived from the general formula (17). Its explicit form is given in appendix B. In figure 4 we show the surface tension and the adsorption density obtained from the reference functional theory together with a fit to the mean-field prediction given by equations (51) and (52). We observe that the latter describes the integral equation results not only close to the coexisting density $\rho_{\mathrm{l}}^* \approx 0.686$ but also up to densities $\rho_0^* = 0.8$ ($\delta\mu^* \approx 1.5$) where we can observe a crossover of the adsorption density from negative to positive values which is equivalent to a maximum in the surface tension. This result is consistent with the idea that the wall–fluid correlations are derived from a generalized mean-field functional; see equation (26) and the discussion thereafter. Note that results very similar to those in figure 4 were obtained in one of the pioneering studies of hard-wall drying [42], in simulations for a square-well fluid.

Next, we compare the predictions for the wall–fluid bridge function $b^{12}(z)$ using the reference functional with those of the reference HNC equations. This comparison is shown in figure 5 for a state point very close to coexistence ($\rho_0^* = 0.6859$) and a state point deep in the stable liquid domain ($\rho_0^* = 0.9$). In reference HNC, the bridge function is derived purely from the reference system (hard spheres with diameter d_1 at the hard wall) and this bridge function is approximated very well by

$$b^{12}_{\mathrm{RHNC}}(z) = \beta \frac{\delta \mathcal{F}^{\mathrm{B,ref}}}{\delta \rho(\mathbf{r})}\bigg|_{\rho(\mathbf{r})=\rho_0 g^{12,\mathrm{ref}}(z)}. \tag{54}$$

Here, $g^{12,\mathrm{ref}}$ is the wall–fluid correlation function for hard spheres at the hard wall obtained by minimizing the Rosenfeld hard-sphere functional in the presence of the hard-wall potential. For the higher bulk density (lower panel in figure 5) b^{12} and b^{12}_{RHNC} show very similar, short-ranged behaviour whereas for the density close to coexistence (upper panel in figure 5) b^{12} acquires a long-ranged component of approximately the same extent as the drying film (compare with the plot of g^{12} in figure 5). Such a long-range behaviour is completely absent in b^{12}_{RHNC} which stays short ranged and consequently the drying film formation is not captured by the reference HNC equations.

3.3. Comparison with the hydrostatic HNC approach

At this point it is worthwhile to compare the present approach with the hydrostatic HNC (HHNC) equations of [11, 12] which is to the author's knowledge the only systematic attempt to account for wetting (drying) phenomena within integral equation theories. Following reference [11], we imagine that an atom of species 2 (originally our hard cavities) exerts a very weak and slowly varying potential on an atom of species 1. Let the slowly varying correlation functions between species 2 and species 1 be denoted by h_{s} and $g_{\mathrm{s}} = h_{\mathrm{s}} + 1$. Then the HHNC bridge function is

$$b^{12}_{\mathrm{HHNC}}(\mathbf{r}) = \beta\mu^{\mathrm{ex}}(\rho_0 g_{\mathrm{s}}(\mathbf{r})) - \beta\mu^{\mathrm{ex}}(\rho_0) - \rho_0 h_{\mathrm{s}}(\mathbf{r}) \frac{\partial(\beta\mu^{\mathrm{ex}})}{\partial\rho}(\rho_0). \tag{55}$$

Here, $\mu^{\mathrm{ex}}(\rho)$ is the excess chemical potential of the fluid (species 1) which is supposed to be known exactly. This expression for the bridge function is exact for slowly varying potentials (hydrostatic limit). Furthermore, we note the thermodynamic identity

$$\rho_0 \frac{(\beta\partial\mu^{\mathrm{ex}})}{\partial\rho}(\rho_0) = -4\pi \int_0^\infty \mathrm{d}r\, r^2 c^{(2)}(r) = -\tilde{c}^{(2)}(0) \tag{56}$$

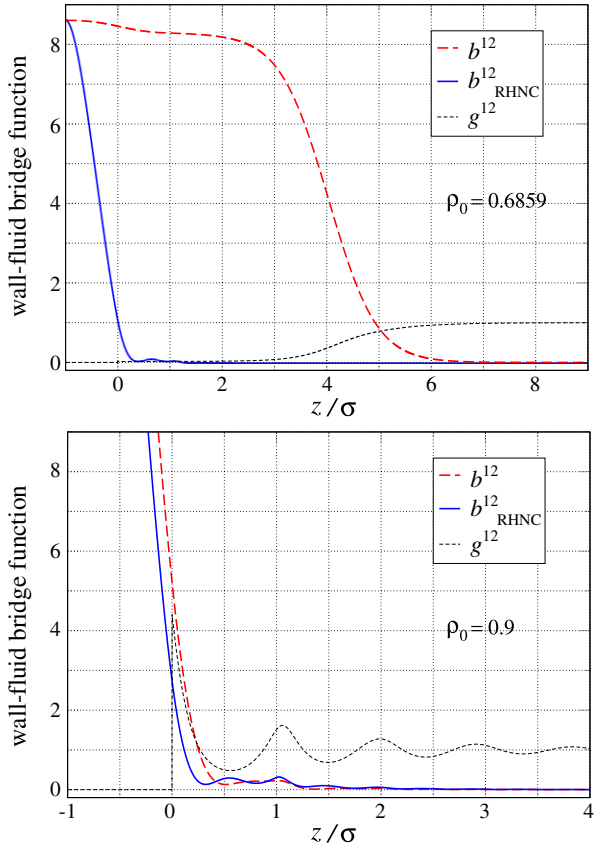

Figure 5. Wall–liquid bridge functions from the reference functional method (thick dashed lines) and reference HNC (thick solid lines) at temperature $T^* = 1.0$. Upper panel: bulk density $\rho_0^* = 0.6859 \approx \rho_l$. Lower panel: bulk density $\rho_0^* = 0.9$. The wall–fluid correlation function g^{12} from the reference functional method is given by the dashed curve. For the density close to coexistence, g^{12} displays a thick drying film whose extent is similar to that of b^{12}, i.e. about 5σ. By contrast, b^{12}_{RHNC} remains short ranged.

which follows from equations (39) and (44). In order to apply this approximation for the bridge function to potentials which vary sharply over molecular distances (i.e., the hard-wall potential or the fluid potential u^{11}) the authors of [11, 12] introduce a normalized weight function $w(\mathbf{r})$ which smoothes the correlation functions:

$$h_s(\mathbf{r}) = w * h^{12}(\mathbf{r}), \qquad g_s(\mathbf{r}) = w * g^{12}(\mathbf{r}). \tag{57}$$

As previously, the asterisk denotes a convolution. Thus the bridge function is

$$b^{12}_{\mathrm{HHNC}}(\mathbf{r}) = \beta\mu^{\mathrm{ex}}(\rho_0 g_s(\mathbf{r})) - \beta\mu^{\mathrm{ex}}(\rho_0) + \rho_0\tilde{c}^{(2)}(0)w * h^{12}(\mathbf{r}). \tag{58}$$

The wall–fluid integral equation based on this bridge function,

$$\log g^{12} + \beta u^{12} = \rho_0 h^{12} * c^{(2)} - b^{12}_{\mathrm{HHNC}} \tag{59}$$

supports a drying solution at the 'true' coexisting densities. To see this, let $\rho_0 = \rho_l$, then within the thick drying film $g^{12} = \rho_g/\rho_l$ and $\beta\mu^{\mathrm{ex}}(\rho_0\, g_s(\mathbf{r})) - \beta\mu^{\mathrm{ex}}(\rho_0) = \log(\rho_l/\rho_g)$, consistent with equation (59). The drawback of this reasoning is that one needs explicitly the function $\mu^{\mathrm{ex}}(\rho)$ (which one would like to actually obtain from the fluid integral equation) and the introduction

of the weight function is purely phenomenological. Furthermore, if one applies this form of the bridge function to the integral equation of the fluid itself, the results are clearly inferior to the present method or to reference HNC. Thus there appears to be no route in HHNC to obtain the excess chemical potential $\mu^{\mathrm{ex}}(\rho)$ self-consistently.

On the other hand, the formally exact bridge function is given by

$$b^{12} = \beta \frac{\delta \mathcal{F}^{\mathrm{B}}}{\delta \rho(\mathbf{r})}\bigg|_{\rho(\mathbf{r})=\rho_0 g^{12}(z)} = \beta\mu^{\mathrm{ex}}[\rho_0 g^{12}(z)] - \beta\mu^{\mathrm{ex}}(\rho_0) + \rho_0 h^{12} * c^{(2)}(z), \tag{60}$$

which follows from equations (7) and (8). Its approximation in the reference functional formalism is given by

$$b^{12} \approx \beta\mu^{\mathrm{ex,ref}}[\rho_0 g^{12}(z); d_1] - \beta\mu^{\mathrm{ex,ref}}(\rho_0; d_1) + \rho_0 h^{12} * c^{(2),\mathrm{ref}}(z; d_1). \tag{61}$$

Here the excess chemical potentials $\mu^{\mathrm{ex}}[\cdot]$ and $\mu^{\mathrm{ex,ref}}[\cdot]$ are given by

$$\mu^{\mathrm{ex[,ref]}}[\rho(\mathbf{r})] = \frac{\delta \mathcal{F}^{\mathrm{ex[,ref]}}}{\delta \rho(\mathbf{r})}. \tag{62}$$

In the case of the Rosenfeld functional, $\mu^{\mathrm{ex,ref}}[\cdot]$ involves double convolutions with a certain set of geometric weight functions (see appendix A). Comparing equations (58) and (61) we note that instead of employing the exact fluid chemical potential μ^{ex} and direct correlation function $c^{(2)}$ the respective reference system quantities appear and that the phenomenological weight function w is replaced by more complicated expressions related to the nature of the reference functional. The comparison illustrates that compared to HHNC the bridge function within the reference functional method takes account of the short-range correlation much better because of the use of the very accurate Rosenfeld functional. On the other hand, through the introduction of the reference system, the hydrostatic limit is not fulfilled by the reference functional method; this is reflected by the fact that the coexisting densities derived from hard-wall drying (equations (49) and (50)) are not perfectly consistent with those from the Maxwell construction.

3.4. Sum rules and the relation to mean-field DFT

For the planar hard-wall problem, two important sum rules exist:

$$\frac{\beta p}{\rho_0} = g^{12}(0), \tag{63}$$

$$-\frac{\partial \gamma_{\mathrm{wl}}}{\partial \mu} = \Gamma_{\mathrm{wl}}(\mu). \tag{64}$$

The first is the contact sum rule (see equation (45)) which links the pressure p in the bulk to the fluid density at contact with the wall. The second (not specific to the hard-wall problem) is the Gibbs adsorption equation and links the surface tension to the adsorption density. As usual, the derivative is performed on an isotherm.

The Gibbs adsorption rule remains valid for local density functionals and functionals which are constructed from weighted densities (WDA). The contact rule remains only valid for free energy functionals of WDA type [27]. This has rendered such functionals a popular tool for the investigation of inhomogeneous matter. However, one should add the proviso that in equation (63) the pressure p is the one derived from the free energy functional for bulk densities, i.e. from the compressibility equation of state. Simple fluids are almost exclusively treated in density functional theory using a mean-field approximation for the attractive tails

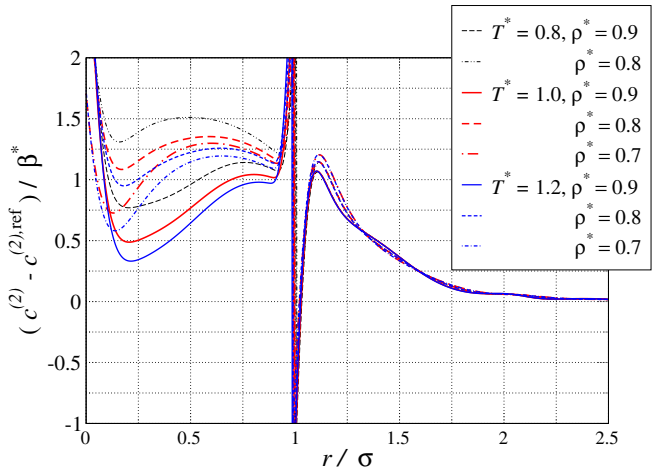

Figure 6. The difference between the direct correlation functions of the fluid and of the reference system for various stable liquid states.

(see below) for which the consistency between the virial and compressibility equations of state is not very good. Moreover, one might object that agreement with sum rule (64) does not guarantee the accuracy of γ_{wl} and Γ_{wl} themselves, as these quantities depend strongly on the quality of the free energy functional.

For hard spheres, these problems are solved to a high degree of accuracy by currently available functionals [26, 45]. The simplest mean-field treatment of fluids in which the pair potential $u^{11}(r)$ has an attractive tail is given by

$$\mathcal{F}^{\mathrm{ex}}[\rho(r)] = \mathcal{F}^{\mathrm{ex,ref}}[\rho(r); d_1 = \mathrm{const}] + \tfrac{1}{2}\int \mathrm{d}\mathbf{r}\, \rho(\mathbf{r}) w_{\mathrm{att}} * \rho(\mathbf{r}), \tag{65}$$

where we consider a one-component system. Here, the weight function w_{att} is given by the attractive tail of the interparticle potential (for which various recipes exist in the literature). If we compare the second term in equation (65) with the excess free energy beyond the reference system in our approach (see equation (26)), then the reference functional approach predicts roughly mean-field behaviour for the *density deviations* from the bulk. Thus we may conclude that if the prefactor of the quadratic term in equation (26), $(c^{(2)} - c^{(2),\mathrm{ref}})/\beta$, does not vary appreciably with the bulk density ρ_0 then a description in terms of the functional given in equation (65) will capture the essential physics. Checking the numerical results (see figure 6), we find that for $r > \sigma$ a single function does indeed describe this prefactor for all stable liquid state points except for the ones in the critical region. Inside the harshly repulsive core ($r < \sigma$) we notice some variation which is, however, small when compared to the magnitude of the direct pair correlation function of the reference system. Thus the 'mean-field' expansion around the bulk density as given in equation (26) is expected to entail similar physics as that in the mean-field functional (65) but the former has the effect of giving a more accurate equation of state and very reliable fluid correlation functions. The mean-field approach (26) is, in turn, computationally less demanding and has the advantage that the sum rules hold analytically (with respect to the compressibility equation of state).

It is important to note that the very concept of expanding around a fixed bulk density implies that the sum rule proofs which work for weighted density functionals do not hold for the Taylor expanded functional [46]. Therefore we have tested both sum rules numerically for various

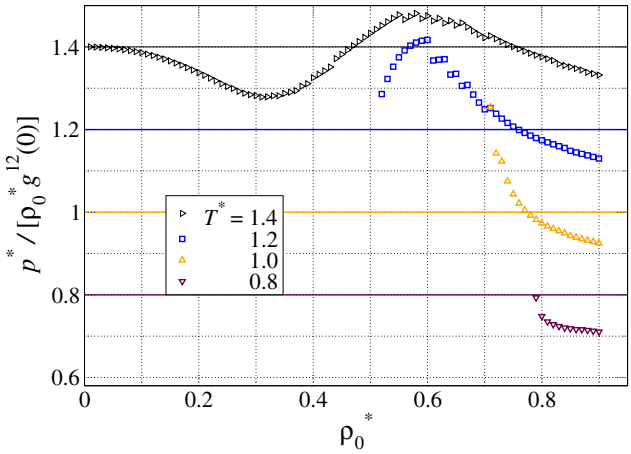

Figure 7. Testing the consistency of the contact density sum rule, equation (63). We have plotted the ratio $p^*/(\rho_0^* g^{12}(0))$ for various temperatures $T^* = 0.8 \cdots 1.4$. The sum rule value of this ratio, T^*, is shown by a horizontal straight line. For the three lowest temperatures, results are plotted for the stable liquid phase only.

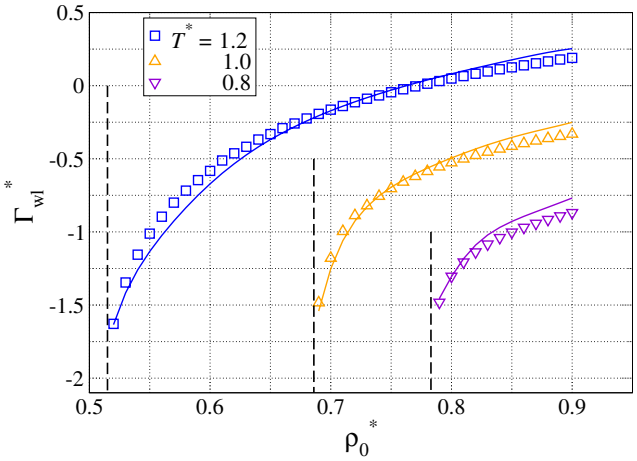

Figure 8. Testing the consistency of the Gibbs adsorption rule, equation (64). We show a comparison of the adsorption density $\Gamma_{wl} = \rho_0 \int dz\, h^{12}$ (symbols) with the same quantity obtained from sum rule (64) as a function of the bulk density for temperatures $T^* = 0.8$, 1.0 and 1.2. To perform the μ derivative of the surface tension γ_{wl}, both μ and γ_{wl} have been fitted to polynomials in ρ_0. The fit is of limited accuracy only very close to coexistence. The vertical dashed lines mark the coexisting liquid densities. For clarity, Γ_{wl}^* has been shifted by -0.5 for $T^* = 1.0$ and -1 for $T^* = 0.8$.

temperatures. In figure 7 we have plotted the ratio of the virial pressure to the density at contact, $p^*/[\rho_0 g^{12}(0)]$ (which should give T^*), for temperatures ranging from $T^* = 0.8 \cdots 1.4$. The deviations are up to 20%. However, despite these deviations these results are encouraging since here the *virial* (= quasi-exact) pressure is used. In figure 8 we compare the adsorption densities calculated by equation (53) with the adsorption density obtained from the surface tension via the sum rule (64). Again we find very reasonable agreement.

4. Summary and conclusions

In this paper, we have analysed the pair correlation functions of an inhomogeneous fluid mixture by means of a functional Taylor expansion of the free energy around an inhomogeneous density profile. We have derived a general integral equation closure for inhomogeneous systems which is based on the introduction of a reference functional for the excess free energy beyond second order in the Taylor expansion. A benefit of this approach is that explicit expressions (see equation (19)) for the insertion free energies of particles into the inhomogeneous equilibrium distribution are obtained, which reduce to explicit expressions for the excess chemical potential if the expansion is performed around a homogeneous (bulk) state.

As an application, we have considered the equation of state for a bulk cut-off and shifted Lennard-Jones fluid and the structure and adsorption of this fluid at a hard wall. Treating this problem within the mixture theory and expanding around the bulk state, we find excellent agreement between the virial and internal energy routes to the equation of state for the fluid and with simulations. Thermodynamic consistency is good for stable state points outside the critical region. By virtue of the underlying hard-sphere reference functional, complete drying is predicted for the hard-wall–liquid interface and the corresponding coexisting densities for the liquid branch are in excellent agreement with those from the Maxwell construction. However, there are deviations for the coexisting densities on the gas branch. Nevertheless, this reasonable consistency between the Maxwell construction and hard-wall drying is a novel result within integral equation approaches.

Two sum rules related to the hard-wall problem, the contact density rule, equation (63), and the Gibbs adsorption, equation (64), have been investigated over a wide range of densities and temperatures. Although these sum rules are not satisfied exactly, the deviations are reasonably small, especially near coexistence.

The numerical results for both the fluid–fluid and the wall–fluid correlations suggest a generalized mean-field behaviour outside the critical region. In the reference functional approach, the difference between the fluid free energy and the free energy of the reference system is expanded up to second order in the density difference (from the bulk density); see equation (26). The coefficient of the second-order term, the difference between the pair direct correlation functions of the fluid and the reference system, is determined self-consistently and turns out to be quite insensitive to variations in temperature and bulk density for liquid states; see figure 6. Therefore, we argue that for physical problems related to wetting and drying a description with density functionals composed of an accurate reference part and a mean-field attractive term should be sufficient to capture all the essential features and will be much less demanding in computational effort.

Related to the efficacy of generalized mean-field treatments of simple fluids, we note that a quite different mean-field treatment of the density deviations from the bulk has already been developed in [47] in which the behaviour of an LJ fluid at a hard wall was studied as well. In contrast to the present study, the properties of the hard-sphere reference system were fixed by considering the first YBG equation; for details see [47]. Good agreement between simulated and calculated density profiles was obtained for selected supercritical state points.

The description of wetting phenomena is also possible within the present approach if for the description of the gas phase a reference system hard-sphere diameter d_1 is chosen which is close to the values needed for the description of the liquid branch (around $1\,\sigma$). This choice is in contrast to the empirical criterion (36) which predicts $d_1 \to 0$ for state points in the gas phase at temperatures $T^* < 1.2$. However, the criterion seems to be of limited use in the gas phase since the thermodynamic properties depend only very weakly on the choice of d_1 there, i.e. the choice $d_1 \sim \sigma$ describes the state points in the gas phase equally well.

We anticipate interesting perspectives for further computations in the problem of small colloidal particles at interfaces. The free energy profile for particles dragged through the interface or their mutual interactions at the interface are only beginning to be understood. These observables can be analysed within the reference functional approach for inhomogeneous distributions; the challenging numerical implementation remains a task for future work.

Acknowledgments

The author is grateful to the Alexander von Humboldt Foundation for a research grant supporting a stay in Bristol during which a good part of this work was completed. He thanks the Physics Department in Bristol and especially Bob Evans and Andy Archer for their hospitality and for enjoyable discussions. Bob Evans has followed the development of the work presented here with great interest and has provided many helpful suggestions and he is also thanked for a thorough reading of the manuscript. Furthermore, the author thanks Roland Roth for beneficial discussions.

Appendix A. The Rosenfeld functional

The Rosenfeld functional [25, 38] describing a mixture of hard spheres with radii R_i is given by

$$\beta\mathcal{F}^{\mathrm{ref}} = \int \mathrm{d}\mathbf{r}\, \Phi(\{\mathbf{n}(\mathbf{r})\}) \tag{A.1}$$

where Φ is a function of a set of weighted densities $\{\mathbf{n}(\mathbf{r})\} = \{n_0, n_1, n_2, n_3, \mathbf{n}_1, \mathbf{n}_2\}$ with four scalar and two vector densities. These are related to the density profile $\rho_i(\mathbf{r})$ of species i by

$$n_\alpha = \sum_i \rho_i * w_i^\alpha(\mathbf{r}), \tag{A.2}$$

and the hereby introduced weight functions for species i, $\{\mathbf{w}(\mathbf{r})\} = \{w_i^0, w_i^1, w_i^2, w_i^3, \mathbf{w}_i^1, \mathbf{w}_i^2\}$, depend on the species radius R_i as follows:

$$\begin{aligned}
&w_i^3 = \theta(R_i - |\mathbf{r}|),\\
&w_i^2(\mathbf{r}) = \delta(R_i - |\mathbf{r}|), \qquad w_i^1(\mathbf{r}) = \frac{w_i^2(\mathbf{r})}{4\pi R_i}, \qquad w_i^0(\mathbf{r}) = \frac{w_i^2(\mathbf{r})}{4\pi R_i^2},\\
&\mathbf{w}_i^2(\mathbf{r}) = \frac{\mathbf{r}}{|\mathbf{r}|}\delta(R_i - |\mathbf{r}|), \qquad \mathbf{w}_i^1(\mathbf{r}) = \frac{\mathbf{w}_i^2(\mathbf{r})}{4\pi R_i}.
\end{aligned} \tag{A.3}$$

Finally, the functional form for the free energy density Φ is given by

$$\Phi(\{\mathbf{n}(\mathbf{r})\}) = -n_0 \ln(1-n_3) + \frac{n_1 n_2}{1-n_3} + \frac{n_2^3}{24\pi(1-n_3)^2} - \frac{\mathbf{n}_1\cdot\mathbf{n}_2}{1-n_3} - \frac{n_2\mathbf{n}_2\cdot\mathbf{n}_2}{8\pi(1-n_3)^2}. \tag{A.4}$$

Appendix B. Surface tension at the hard wall

The hard-wall–liquid surface tension is defined by the expression

$$\gamma_{\mathrm{wl}} = \int_0^\infty \mathrm{d}z\, (\omega(z) + p), \tag{B.1}$$

where $\omega(z)$ is the grand potential volume density and $p = p(\rho_0)$ is the bulk pressure of the liquid with density ρ_0. In terms of the grand potential density functional, this equation is equivalent to

$$\gamma_{\mathrm{wl}} = \left(\Omega[\rho(\mathbf{r})]|_{\rho(\mathbf{r})=\rho_0 g^{12}(z)} - \Omega[\rho(\mathbf{r})]|_{\rho(\mathbf{r})=\rho_0\theta(z)}\right)/A, \tag{B.2}$$

where A denotes the area of the wall. We use the definition

$$\Omega[\rho(\mathbf{r})] = \mathcal{F}[\rho(\mathbf{r})] - \int \mathrm{d}\mathbf{r}\,(\mu(\rho_0) - \xi u^{12}(\mathbf{r}))\rho(\mathbf{r}) \tag{B.3}$$

with $\xi = 1$ for the first term in equation (B.2) and $\xi = 0$ for the second term. According to the discussion below equation (35) concerning the hard-wall limit, the functional of the free energy is the functional for the one-component LJ fluid,

$$\mathcal{F}[\rho(\mathbf{r})] = \mathcal{F}^{\mathrm{id}}[\rho(\mathbf{r})] + \mathcal{F}^{\mathrm{HNC}}[\rho(\mathbf{r})] + \mathcal{F}^{\mathrm{B,ref}}[\rho(\mathbf{r}); d_1], \tag{B.4}$$

with $d_1 = d_1(\rho_0)$ denoting the reference system hard-sphere diameter. Straightforward evaluation gives

$$\beta\gamma_{\mathrm{wl}} = \int_0^\infty \mathrm{d}z\,\rho_0 \left(g^{12}\ln g^{12} - h^{12}(1 + \beta\mu^{\mathrm{ex,ref}}(\rho_0)) - \frac{\rho_0}{2}\left[(c_z^{(2)} - c_z^{(2),\mathrm{ref}}) * h^{12}\right] h^{12} \right)$$
$$+ \beta\mathcal{F}^{\mathrm{ex,ref}}[\rho_0 g^{12}] - \beta\int_0^\infty \mathrm{d}z\, f^{\mathrm{ex,ref}} + I_{\mathrm{wall}}, \tag{B.5}$$

$$I_{\mathrm{wall}} = \int_{-\infty}^0 \mathrm{d}z \left(\beta[f^{\mathrm{ex}}(\rho_0) - f^{\mathrm{ex,ref}}(\rho_0)] \right.$$
$$\left. + \rho_0 h^{12}\beta(\mu^{\mathrm{ex}}(\rho_0) - \mu^{\mathrm{ex,ref}}(\rho_0)) - \frac{\rho_0^2}{2}\left[(c_z^{(2)} - c_z^{(2),\mathrm{ref}}) * h^{12}\right] h^{12} \right). \tag{B.6}$$

Here, $f^{\mathrm{ex}}(\rho_0)$ and $f^{\mathrm{ex,ref}}(\rho_0)$ are the bulk free energy volume densities of the fluid and the hard-sphere reference system, respectively. We note that the non-local expansion of the free energy in terms of $\Delta\rho = \rho_0 h^{12}$ ($=-\rho_0$ for $z < 0$) introduces contributions inside the wall, contained in I_{wall}. Furthermore,

$$c_z^{(2)[,\mathrm{ref}]}(z) = 2\pi\int_{|z|}^\infty r\,\mathrm{d}r\, c^{(2)[,\mathrm{ref}]}(r), \tag{B.7}$$

and we have introduced the one-dimensional convolution

$$c_z^{(2)[,\mathrm{ref}]} * h^{12}(z) = \int_{-\infty}^\infty \mathrm{d}z'\, c_z^{(2)[,\mathrm{ref}]}(z - z')h^{12}(z'). \tag{B.8}$$

The unknown free energy density of the liquid $f^{\mathrm{ex}}(\rho_0)$ appearing in the integral I_{wall} is fixed by the requirement that beyond the wall ($z < 0$) the density is zero and therefore also $f^{\mathrm{ex}}(0) = 0$. On the other hand, $f^{\mathrm{ex}}(0)$ is determined by the functional Taylor expansion of the fluid excess free energy around ρ_0, evaluated at zero density. Therefore, we find

$$f^{\mathrm{ex}}(\rho_0) = f^{\mathrm{ex,ref}}(\rho_0) + \rho_0(\mu^{\mathrm{ex}}(\rho_0) - \mu^{\mathrm{ex,ref}}(\rho_0)) + \frac{\rho_0^2}{2}\left[\tilde{c}^{(2)}(0) - \tilde{c}^{(2),\mathrm{ref}}(0)\right]. \tag{B.9}$$

This expression is inserted into I_{wall} and we obtain the expression

$$I_{\mathrm{wall}} = \frac{\rho_0^2}{2}\int_{-\infty}^0 \mathrm{d}z\,\left(\left[\tilde{c}^{(2)}(0) - \tilde{c}^{(2),\mathrm{ref}}(0)\right] - \left[(c_z^{(2)} - c_z^{(2),\mathrm{ref}}) * h^{12}\right] h^{12}\right). \tag{B.10}$$

This completes the prescription for calculating γ_{wl}.

References

[1] Morita T and Hiroike K 1960 *Prog. Theor. Phys.* **23** 1003

[2] Stell G 1964 *The Equilibrium Theory of Classical Fluids* ed H L Frisch and J L Lebowitz (New York: Benjamin) p II-171

[3] Percus J K 1964 *The Equilibrium Theory of Classical Fluids* ed H L Frisch and J L Lebowitz (New York: Benjamin) p II-33

[4] Pastore G, Akinlade O, Matthews F and Badirkhan Z 1998 *Phys. Rev.* E **57** 460
[5] Parola A and Reatto L 1995 *Adv. Phys.* **44** 211
[6] Pini D and Stell G 2002 *Physica* A **306** 270
[7] Vompe A G and Martynov G A 1996 *J. Chem. Phys.* **106** 6095
[8] Lado F, Foiles S M and Ashcroft N W 1983 *Phys. Rev.* A **28** 2374
[9] Hansen J-P and McDonald I 1990 *Theory of Simple Liquids* (London: Academic)
[10] Evans R, Tarazona P and Marconi U M B 1983 *Mol. Phys.* **50** 993
[11] Zhou Y and Stell G 1990 *J. Chem. Phys.* **92** 5533
[12] Zhou Y and Stell G 1990 *J. Chem. Phys.* **92** 5544
[13] Kjellander R and Sarman S 1989 *J. Chem. Phys.* **90** 2768
[14] Kjellander R and Sarman S 1990 *Mol. Phys.* **70** 215
[15] Nieminen R and Ashcroft N W 1981 *Phys. Rev.* A **24** 560
[16] McGough R A and Miller M D 1986 *Phys. Rev.* A **34** 457
[17] Plischke M and Henderson D 1986 *J. Chem. Phys.* **84** 2846
[18] Bruno E, Caccamo C and Tarazona P 1987 *Phys. Rev.* A **35** 1210
[19] Orlandi A, Parola A and Reatto L 2004 A microscopic approach to critical phenomena at interfaces: an application to complete wetting in the Ising model *Preprint* cond-mat/0409188
[20] Ebner C and Saam W F 1977 *Phys. Rev. Lett.* **38** 1486
[21] Evans R 1992 *Fundamentals of Inhomogeneous Fluids* ed D Henderson (New York: Dekker) pp 85–175
[22] Evans R and Tarazona P 1983 *Phys. Rev.* A **28** 1864
[23] Kroll D M and Meister T F 1985 *Phys. Rev.* B **31** 392
[24] Tarazona P 1985 *Phys. Rev.* A **31** 2672
[25] Rosenfeld Y 1989 *Phys. Rev. Lett.* **63** 980
[26] Roth R, Evans R, Lang A and Kahl G 2002 *J. Phys.: Condens. Matter* **14** 12063
[27] van Swol F and Henderson J R 1989 *Phys. Rev.* A **40** 2567
[28] Choudhury N and Ghosh S 2001 *J. Chem. Phys.* **114** 8530
[29] Gillespie D, Nonner W and Eisenberg R S 2003 *Phys. Rev.* E **68** 031503
[30] Tang Y and Wu J 2003 *J. Chem. Phys.* **119** 7388
[31] Rosenfeld Y 1993 *J. Chem. Phys.* **98** 8126
[32] Rosenfeld Y 1996 *Phys. Rev.* E **54** 2827
[33] Rosenfeld Y 1998 *Mol. Phys.* **94** 929
[34] Evans R 1979 *Adv. Phys.* **28** 143
[35] Henderson J R 1983 *Mol. Phys.* **50** 741
[36] Brader J M, Evans R and Schmidt M 2003 *Mol. Phys.* **101** 3349
[37] Schmidt M 2004 *J. Phys.: Condens. Matter* **16** L351 (*Preprint* cond-mat/0407013)
[38] Kahl G, Bildstein B and Rosenfeld Y 1996 *Phys. Rev.* E **54** 5391
[39] Oettel M 2004 *Phys. Rev.* E **69** 041404
[40] Cuesta J A, Martinez-Raton Y and Tarazona P 2002 *J. Phys.: Condens. Matter* **14** 11965
[41] Johnson J K, Zollweg A and Gubbins K E 1993 *Mol. Phys.* **78** 591
[42] Henderson J R and van Swol F 1985 *Mol. Phys.* **56** 1313
[43] Evans R, Henderson J R and Roth R 2004 *J. Chem. Phys.* **121** 12074
(Evans R, Henderson J R and Roth R 2004 Non-analytic curvature contributions to solvation free energies: influence of drying *Preprint* cond-mat/0410179)
[44] Dietrich S 1988 *Phase Transitions and Critical Phenomena* vol 12, ed C L Domb and J L Lebowitz (London: Academic) p 1
[45] Bryk P, Roth R, Mecke K R and Dietrich S 2003 *Phys. Rev.* E **68** 031602
[46] Sweatman M B 2000 *Mol. Phys.* **98** 573
[47] Weeks J D, Katsov K and Vollmayr K 1998 *Phys. Rev. Lett.* **81** 4400